Short duration of Early Permian Qiangtang-Panjal large igneous province: Implications for origin of the Neo-Tethys Ocean

Wei Dan [a,b,*], Qiang Wang [a,b,c], J. Brendan Murphy [d,e], Xiu-Zheng Zhang [a,b], Yi-Gang Xu [a,b,c], William M. White [f], Zi-Qi Jiang [g], Quan Ou [a,h], Lu-Lu Hao [a,b], Yue Qi [a,b]

[a] State Key Laboratory of Isotope Geochemistry, Guangzhou Institute of Geochemistry, Chinese Academy of Sciences, Guangzhou 510640, China
[b] CAS Center for Excellence in Deep Earth Science, Guangzhou 510640, China
[c] College of Earth and Planetary Sciences, University of Chinese Academy of Sciences, Beijing 10049, China
[d] Department of Earth Sciences, St Francis Xavier University, PO Box 5000, Antigonish, Nova Scotia, B2G 2W5 Canada
[e] Earth Dynamics Research Group, The Institute for Geoscience Research (TIGeR), School of Earth and Planetary Sciences, Curtin University, WA 6845, Australia
[f] Department of Earth and Atmospheric Sciences, Cornell University, Ithaca, NY 14853, USA
[g] School of Earth Science, Guilin University of Technology, Guilin 541004, China
[h] State Key Laboratory of Oil and Gas Reservoir Geology and Exploitation, Institute of Sedimentary Geology, Chengdu University of Technology, Chengdu 610059, China

ARTICLE INFO

ABSTRACT

Northward drift of the Cimmerian microcontinents and opening of the Neo-Tethys Ocean in Early Permian are prominent events in northern Gondwana's protracted breakup history. However, the geodynamic setting responsible for these events is controversial. The dispersal of the eastern Cimmerian microcontinents was accompanied by the emplacement of Qiangtang-Panjal large igneous province (QP-LIP). Previously published zircon U-Pb data imply the QP-LIP was emplaced over a long interval (320-280 Ma) but are inconsistent with the short eruption interval constrained by biostratigraphic studies. New secondary ion mass spectrometry (SIMS) zircon U-Pb ages from 15 mafic dikes and gabbroic intrusions from the Southern Qiangtang terrane as well as age data from other parts of the QP-LIP show a much shorter duration ($\sim 290 - 285$ Ma) for this LIP. The QP-LIP was characterized by an initial ~ 290 Ma alkalic and tholeiitic phases and a subsequent ~ 285 Ma tholeiitic phase, in agreement with regional biostratigraphic data constraining the timing of departure of the eastern Cimmerian microcontinents from Gondwana at ~ 285 Ma and the opening of the Neo-Tethys Ocean. The QP-LIP was most likely the consequence of the arrival in the upper mantle of a mantle plume beneath the northern Gondwanan margin. This event, in combination with slab pull associated with subduction beneath Laurasia, may have caused extension and rifting of east Cimmerian continental fragments from the northern margin of Gondwana. This study may elucidate the mechanism responsible for repeated episodes of one-way northward drifting terranes from northern Gondwana that commenced in Paleozoic.

© 2021 Elsevier B.V. All rights reserved.

1. Introduction

It has been long recognized that terrane separation from northern Gondwana and accretion to Eurasia occurred in repeated episodes beginning in the Late Silurian (Stampfli and Borel, 2002; Metcalfe, 2013; Wu et al., 2020). These episodes were accompanied by the opening and closing of the Paleo-Tethys and Neo-Tethys oceans, which are important features in late Paleozoic-early Meso-zoic paleocontinental reconstructions (Stampfli and Borel, 2002; Torsvik et al., 2006). The geodynamic scenario responsible for repeated one-way northward drifting of terranes is enigmatic. As the oceanic slab subducted northward beneath Eurasia, concomitant slab pull forces are commonly inferred to be dominant (e.g., Stampfli and Borel, 2002; Gutiérrez-Alonso et al., 2008; Wan et al., 2019; Wu et al., 2020). However, recent evidence suggests that a large low shear wave velocity province (LLSVP), which may drift slowly (e.g., Flament et al., 2017), existed beneath Pangea in the late Paleozoic. As mantle plumes are preferentially generated along the margins of LLSVPs, they may have played an important role in rifting the terranes from the northern Gondwanan margin (Torsvik et al., 2006; Burke et al., 2008). However, as these terranes were complexly deformed and their contiguity was severed during

their accretion to Eurasia, the correlation of major tectonothermal events between their constituent blocks is challenging. Such challenges make it difficult to assess the role of mantle plumes in the separation of terranes from the northern Gondwanan margin (Wan et al., 2019; Wu et al., 2020).

The timing, geodynamic setting and even the existence of the Paleo-Tethys Ocean are controversial (e.g., Stampfli and Borel, 2002; Metcalfe, 2013; Wu et al., 2020). However, the formation of the younger Neo-Tethys Ocean is much better constrained and is commonly interpreted as one of the earliest stages in the breakup of Gondwana (e.g., Stampfli and Borel, 2002). Opening of the Neo-Tethys Ocean in the Permian was accompanied by northward drift of the Cimmerian microcontinents (presently dispersed from Turkey to SE Asia) from the northern margin of Gondwana (Stampfli and Borel, 2002; Metcalfe, 2013). Based on documentation of ongoing subduction beneath Eurasia during northward migration of Cimmerian microcontinents, it has long been suggested that slab pull related to subduction of the Paleo-Tethys oceanic slab beneath Eurasia is responsible for opening of the Neo-Tethys Ocean (Stampfli and Borel, 2002; Gutiérrez-Alonso et al., 2008).

Rifting that heralded the departure of the Cimmerian terranes from the northern Gondwanan margin was accompanied by emplacement of vast volumes of mafic rocks, interpreted as a Large Igneous Province (LIP) in northern Gondwana (Zhai et al., 2013; Ernst, 2014; Liao et al., 2015). This interpretation raises the possibility that a mantle plume may have played a significant role in the opening of the Neo-Tethys Ocean. In addition, the timing of this putative LIP event relative to the retreat of the late Paleozoic Gondwanan ice sheets has been emphasized in studies examining the relationship between plume activity and climate change (e.g., Wopfner and Jin, 2009). However, detailed geochemical studies focused on the Panjal Traps in the western Himalayas, purported to be a local representative of the LIP, found no solid evidence to support the existence of a mantle plume (e.g., Shellnutt et al., 2015; Yeh and Shellnutt, 2016; Shellnutt, 2018).

As Early Permian rift-related magmatic rocks were widely dispersed by subsequent tectonic events, the original distribution and duration remain poorly constrained. As a result, the relationship of magmatism with opening of the Neo-Tethys Ocean is poorly understood (e.g., Garzanti et al., 1994; Garzanti and Sciunnach, 1997; Yeh and Shellnutt, 2016). In this study, we provide new SIMS zircon U-Pb and geochemical data that tightly constrain the duration of this putative LIP event as well as its chemical evolution and discuss the implications of these data for geodynamic models of the rifting of eastern Cimmerian microcontinents and opening of the Neo-Tethys.

2. Previous dating in the Himalaya-Tibetan Plateau

Early Permian mafic rocks are widely distributed in the Himalaya-Tibetan Plateau, and previous studies in the Himalaya, Lhasa, Southern Qiangtang (SQT) and Baoshan (part of Sibumasu) terranes indicate they may constitute a LIP (Fig. 1a) (e.g., Zhai et al., 2013; Ernst, 2014; Liao et al., 2015). Permian volcanic rocks are documented in the western Himalaya as the Panjal Traps (summarized in Shellnutt, 2018), and this magmatic province has an areal extent of $> 10^4$ km^2. Early Permian igneous rocks occur mainly as mafic lavas, sills and dikes in the SQT and Baoshan terranes. The mafic lavas have an average thickness of ~ 800 m (maximum up to ~ 2000 m) over an area of $\sim 1.41 \times 10^5$ km^2 (based on Zhang and Zhang, 2017), and are $\sim 300 - 500$ m thick over an area of $\sim 0.12 \times 10^5$ km^2 (Liao et al., 2015), respectively. The dikes in the SQT are tens of meters in width and are generally oriented parallel to the continental margin (Zhai et al., 2013). In the Lhasa terrane, a few basalts are interbedded with Lower Permian strata with thickness varying from ~ 80 m to 2 m (Zhu et al., 2010). Taken to-

gether, Early Permian mafic rocks are preserved over an area of $\sim 1.6 \times 10^5$ km^2 in the Himalaya-Tibetan Plateau, satisfying one of the requirements in the definition of a LIP (i.e. $> 1 \times 10^5$ km^2; Coffin and Eldholm, 1994; Bryan and Ernst, 2008; Ernst, 2014). This Early Permian magmatic province in northern Gondwana has been referred to by several different names in the literature, such as Himalayan (Neo-Tethys) event or Himalayan magmatic province (cf., Shellnutt, 2018). In this study, we adopt the term Qiangtang-Panjal large igneous province (QP-LIP) (Ernst, 2014), after the occurrence of the largest preserved remnant in the Qiangtang area and the well-known Panjal Traps. This term explicitly suggests evidence of the LIP is preserved in two major regions whose separation reflects subsequent tectonic activity associated with the northward drift of the Cimmerian terranes and their subsequent orogenesis during their accretion to Eurasia.

Detailed biostratigraphic data from several localities in the Himalayas have long indicated that the eruption of the Panjal Traps occurred in the late Early Permian (Artinskian-Kungurian, 290-273 Ma) (Garzanti et al., 1996, 1999). This interpretation is supported by a ~ 289 Ma U-Pb age (LA-ICPMS zircon) from interbedded rhyolite in the Panjal Traps (Shellnutt et al., 2011). Although the depositional age of the basaltic lavas in the Baoshan terrane is constrained to mid-Artinskian by biostratigraphic data from interbedded strata (Wang et al., 2001), LA-ICPMS zircon U-Pb ages of 310-280 Ma were obtained for mafic dikes (Liao et al., 2015; Liu et al., 2020) suggesting a longer duration for this magmatic event than previously envisaged. Similarly, in the SQT, biostratigraphic studies indicate that the basaltic lavas were emplaced during the Sakmarian (295-290 Ma) (Zhang et al., 2012), whereas LA-ICPMS and SHRIMP zircon U-Pb age data from mafic dikes that intruded these strata suggest a longer (320-280 Ma) duration of magmatism (Zhai et al., 2013; Wang et al., 2019).

3. Samples and methods

In this study, we selected 15 samples, including 10 mafic dikes and 5 small gabbroic intrusions (13GZ70, 72, 75 and 13ZB159, 170) from a large area in the SQT for geochemical analysis and SIMS U-Pb zircon dating (Fig. 1b). Details of the methods used for major and trace element analyses and for zircon U-Pb dating are both provided in the supplement. Previous studies suggest that basaltic lavas in the QP-LIP are mostly tholeiitic, and alkalic compositions were reported only in the western part of the SQT (Xu et al., 2016).

4. Results

Apart from one basaltic andesite (13GZ70) with anomalously high SiO$_2$ (55.9 wt. %), other samples are basalts (44.1-50.3 wt.% SiO$_2$) (Table S1). Four basalts are alkalic (15ZB43, 15ZB54, 15ZB08, 15QT20), and the remainder are tholeiitic (Fig. S1). All samples display enrichment in light rare earth elements (REE) (La$_N$/Yb$_N$ = $6.5 - 17.7$) and lack Eu anomalies. Relative to primitive mantle, the samples exhibit variable Nb, Ta and Ti, with either slight enrichment or depletion (Fig. S1).

Zircon grains separated from these mafic rocks in the SQT (Fig. 1b) exhibit either weak or broad oscillatory zoning (Fig. S2). They have highly variable U and Th contents (Table S2), but high Th/U ratios (0.28-8.12, mostly > 1.0) indicating a magmatic origin. A total of 192 U-Pb analyses were obtained on 190 zircon grains from 15 samples. Except for two older dates that are interpreted as xenocrysts (~ 650 Ma), all yield Early Permian dates between 291 ± 4 Ma and 283 ± 3 Ma (Fig. S2; also shown in Fig. 2b). Zircon grains from a previously recognized alkalic basalt (sample 15ZB54) have a weighted age of 290 ± 2 Ma. Three samples from small gabbroic intrusions (tholeiitic) south of the Yulinshan area also have
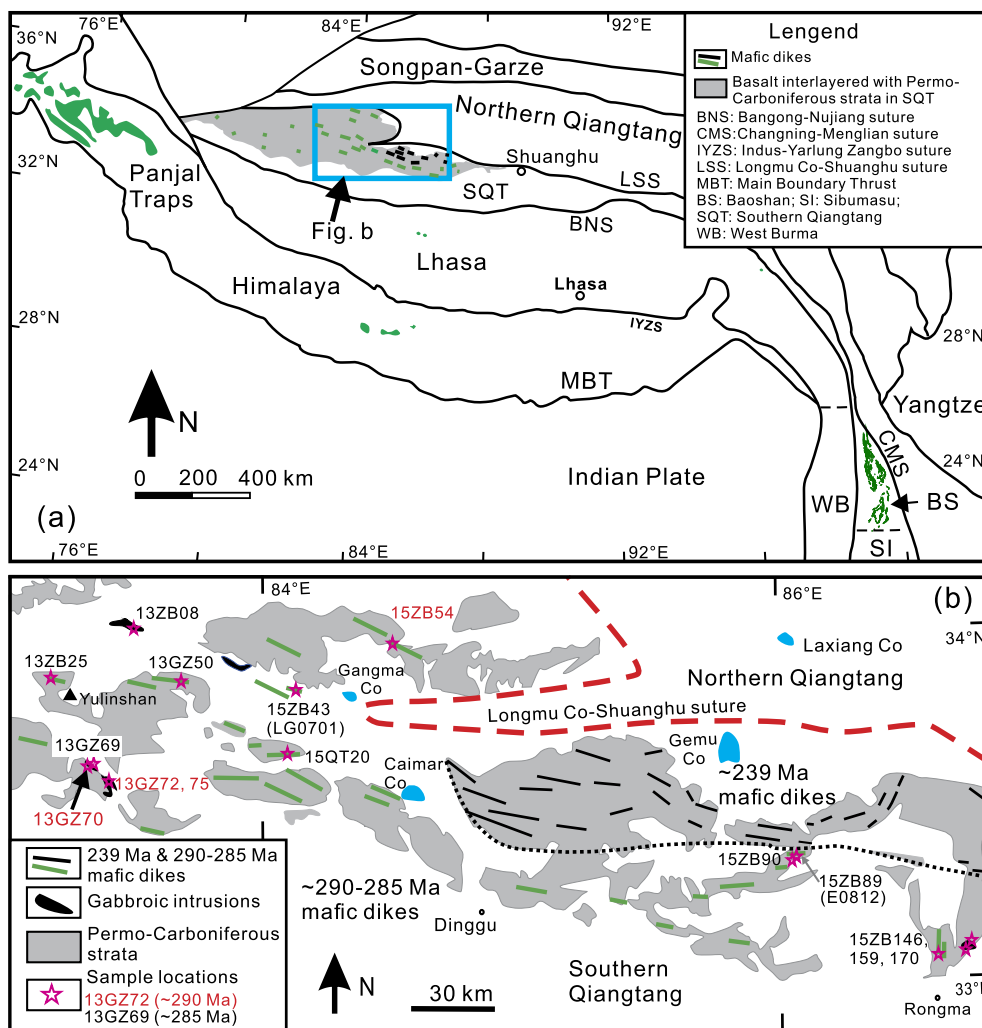
Fig. 1. Simplified geological map for the QP-LIP. (a) The QP-LIP distributed in the Himalaya-Tibetan Plateau (compiled from Zhu et al., 2010; Liao et al., 2015; Shellnutt, 2018; Wang et al., 2019). (b) Geological map of the SQT mafic dikes in Tibet and dating ages for the QP-LIP. The dashed black line separates the ∼ 290 − 285 Ma mafic dikes shown in green from the ∼ 239 Ma shown in black (Dan et al., 2021). Two previous dated samples (Zhai et al., 2013) are included with sample numbers in parentheses (For interpretation of the colors in the figure(s), the reader is referred to the web version of this article.)

weighted ages of ∼ 290 Ma. The remaining 11 samples, including one gabbro and 9 mafic dikes, have ages from 286 ± 3 Ma to 283 ± 3 Ma. Zircon grains from samples 15ZB159 and 15ZB170 have undergone Pb loss, but their intercept dates are within the same age range.

It is noteworthy that two outlier zircon U-Pb ages previously dated by SHRIMP were resampled in the same locations (Fig. 1b). These samples (15ZB43 and 15ZB89) yielded ages of 285 ± 2 Ma and 286 ± 2 Ma, compared with previous SHRIMP dates of 302 ± 2 Ma and 279 ± 1 Ma (Table S3; also see Zhai et al., 2013), respectively. These two outlier ages are therefore considered spurious, and the new SIMS ages are adopted in the following discussion.

5. Discussion

5.1. Duration of the QP-LIP

Over the past decade, published zircon U-Pb ages for the QP-LIP igneous rocks suggested emplacement between 320 and 280 Ma (Fig. 2a), an unusually long time interval for a LIP, for which the overwhelming majority of magmatism is less than 5 Myr in duration, although lifespans of up to ∼ 50 Myr have been documented (Bryan and Ernst, 2008; Ernst, 2014). However, most of these data were obtained by the LA-ICPMS method. Although

the LA-ICPMS, SIMS and SHRIMP methods have similar precision (∼ 1%), LA-ICPMS has significantly less accuracy (∼ 4%) than either SIMS or SHRIMP (∼ 1%) (Li et al., 2015). Thus, to more precisely constrain the duration of the QP-LIP, only the new SIMS ages and previous SHRIMP ages are considered herein.

Collectively, these data yield seventeen high-precision U-Pb ages for mafic rocks in the SQT. They suggest two clusters, i.e., ∼ 291 − 290 Ma, with a peak at ∼ 290 Ma, and ∼ 286 − 283 Ma, with a peak at ∼ 285 Ma (Fig. 2b). The older ∼ 290 Ma phase includes both alkalic and tholeiitic basalts that are exposed in a restricted area of the western part of SQT (Xu et al., 2016; this study), whereas the younger ∼ 285 Ma phase is dominated by tholeiitic basalts that are more widely distributed in the SQT (Zhai et al., 2013; this study). The ∼ 290 Ma phase should occur in the Panjal Traps, as it is the center of the QP-LIP (see Part 5.2). This suggestion is supported by one CA-ID-TIMS zircon age of 288 Ma for a tholeiitic basalt from the Panjal Traps (J.G. Shellnutt, personal communication), which further implies the majority of Panjal Traps formed during this phase. The mafic rocks with less accurate LA-ICPMS ages of 320-280 Ma are tholeiitic in the Baoshan and Lhasa terranes. These samples are located far from the Panjal Traps compared with the SQT (see part 5.2). These characteristics imply they were probably mostly formed in the younger phase. More accurate
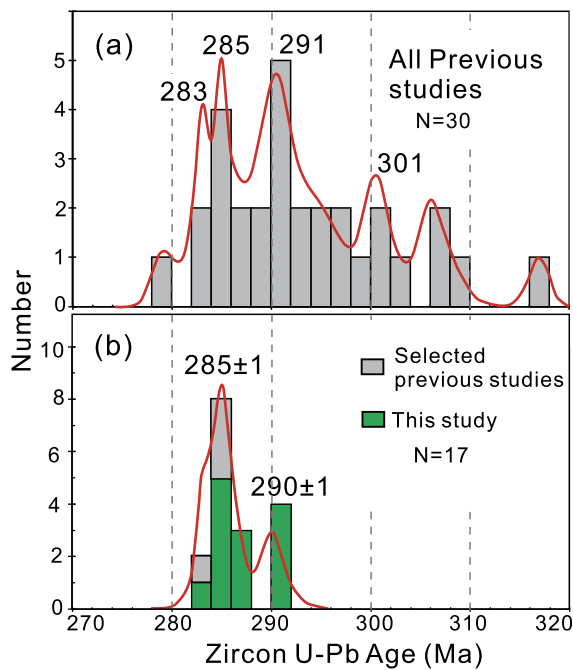
Fig. 2. Zircon U-Pb dating ages for the QP-LIP. (a) All previous zircon U-Pb ages. (b) New SIMS and selected SHRIMP zircon U-Pb ages from SQT mafic dikes. The age data are compiled in Table S3.

Fig. 3. Paleogeographic reconstruction of the Cimmerian microcontinents in the Early Permian (modified from Metcalfe, 2013). The shaded area depicts the effect area of the QP-LIP, and the red circle indicates its center. Terranes with outlined by green color indicate Cimmerian microcontinents.
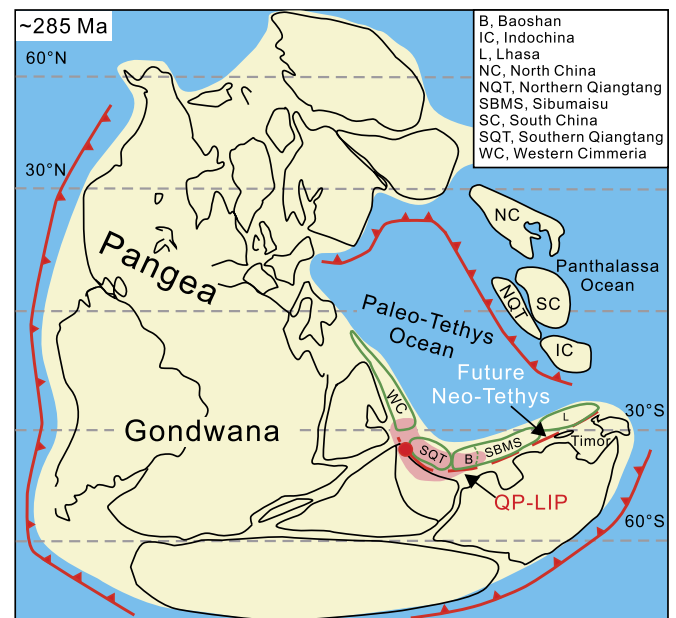
dating outside the SQT is required to reveal which phase is the major magmatic pulse.

These new U-Pb age data for the QP-LIP yield ages are consistent with regional biostratigraphic studies. Many studies from the Himalaya, Baoshan and Lhasa terranes constrain the major eruption period of basaltic lavas to the Artinskian (290-283 Ma) (Himalaya) (Garzanti et al., 1996, 1999), mid-Artinskian (Baoshan) (Wang et al., 2001) or Sakmarian-Artinskian (Zhu et al., 2010) stages. Mafic rocks hosted by Zhanjin Formation in the SQT were previously thought to be lavas and constrained to Sakmarian (294-290 Ma) on the basis of biostratigraphic studies on adjacent strata (Liang et al., 1983; Zhang et al., 2012). However, these mafic rocks have textures typical of diabase (Liang et al., 1983) and are likely to be sills and hence younger than the biostratigraphic age.

There are several examples of mafic rocks in northern Gondwana that are presumed to have been emplaced in the Permian (e.g., Oman and Himalaya). On the basis of geochemical comparisons, these mafic rocks were commonly considered to be temporally correlated to Early Permian rifting event (e.g., Yeh and Shellnutt, 2016; Rehman et al., 2018; Shellnutt, 2018). Middle Permian ($\sim 270 - 260$ Ma) mafic rocks were reported as basalts in Oman (e.g., Lapierre et al., 2004), and mafic dikes/lavas (Zhu et al., 2010) or as protoliths of Cenozoic eclogites formed during the India-Lhasa collision (e.g., Rehman et al., 2018) in the Himalaya. However, the rifting of SQT from northern Gondwana coincides with the opening of the Neo-Tethys Ocean at ~ 285 Ma (see section 5.4), implying the 270-260 Ma magmatism is not related to the QP-LIP. This Middle Permian magmatism reflects either post-rifting magmatism after ocean opening or another phase of extension along the northern margin of Gondwana. In addition, the Abor volcanic rocks in the eastern Himalaya were recently dated at ~ 132 Ma (Singh et al., 2020), implying they cannot be related to the QP-LIP.

5.2. Reconstruction of the east Cimmerian microcontinents and QP-LIP

The QP-LIP was fragmented by the departure of the east Cimmerian terranes accompanying opening of the Neo-Tethys Ocean and by subsequent orogenesis during terrane accretion (Metcalfe, 2013). As a result of these complexities, the original distribution of the QP-LIP has not been precisely reconstructed. Fortunately, the location and evolution of most of the terranes of east Cimmeria have been well-constrained by paleontology, paleoclimatology, paleography and paleomagnetic data (Metcalfe, 2013), allowing for a relatively precise Early Permian reconstruction (Fig. 3). For example, most studies show the Baoshan-Sibumasu terrane as the eastern extension of the SQT and located outboard of west Australia (Metcalfe, 2013). Their proximity to one another and to India-Australia is supported by their similar Early Permian lithologies including glacial-marine diamictite, shale, mudstone and sandstone (Fig. S3) and, as revealed in this study, a distinctively short interval ($\sim 290 - 285$ Ma) of mafic magmatism.

The geological evolution of the Lhasa terrane is enigmatic. It is located between the major subdomains of the LIP (Southern Qiangtang and Himalaya terranes) in present Himalaya-Tibetan Plateau and has a relatively low volume of Early Permian basalts. Most reconstructions follow Zhu et al. (2011) in positioning the Lhasa terrane adjacent to Australia. We further propose that the Lhasa terrane was located at the easternmost part of the Cimmerian terranes (eastern extension of the Baoshan-Sibumasu and adjacent to north Australia) based on recent paleomagnetic data, which implies a location at a low paleolatitude ($16.9° \pm 7.8°$S) during late Early Permian (Kungurian, ~ 275 Ma), significantly north of the Baoshan-Sibumasu terrane at ~ 285 Ma ($41.9° \pm 8.5°$S), but similar in latitude to Baoshan-Sibumasu terrane during Middle Permian (~ 265 Ma) ($13.3° \pm 1.6°$S) (Table S4). In contrast, a location of the Lhasa terrane to the south of the Baoshan-Sibumasu terrane would require the Lhasa terrane to have moved northward at an implausibly high velocity of ~ 28 cm/yr from ~ 285 Ma ($\sim 41.9°$S) to ~ 275 Ma ($\sim 16.9°$S), but then to become relatively immobile with velocity of 0.4 cm/yr from ~ 275 Ma ($\sim 16.9°$S) to ~ 265 Ma ($\sim 13.3°$S). Thus, we conclude that Lhasa terrane was more likely located along the eastern part of the Cimmerian terranes, adjacent to north Australia in the Early Permian (Fig. 3).

This reconstruction of the east Cimmerian microcontinents and QP-LIP is supported by the distribution of basalts with different thickness in each terrane. The cumulative thickness of the basalts,
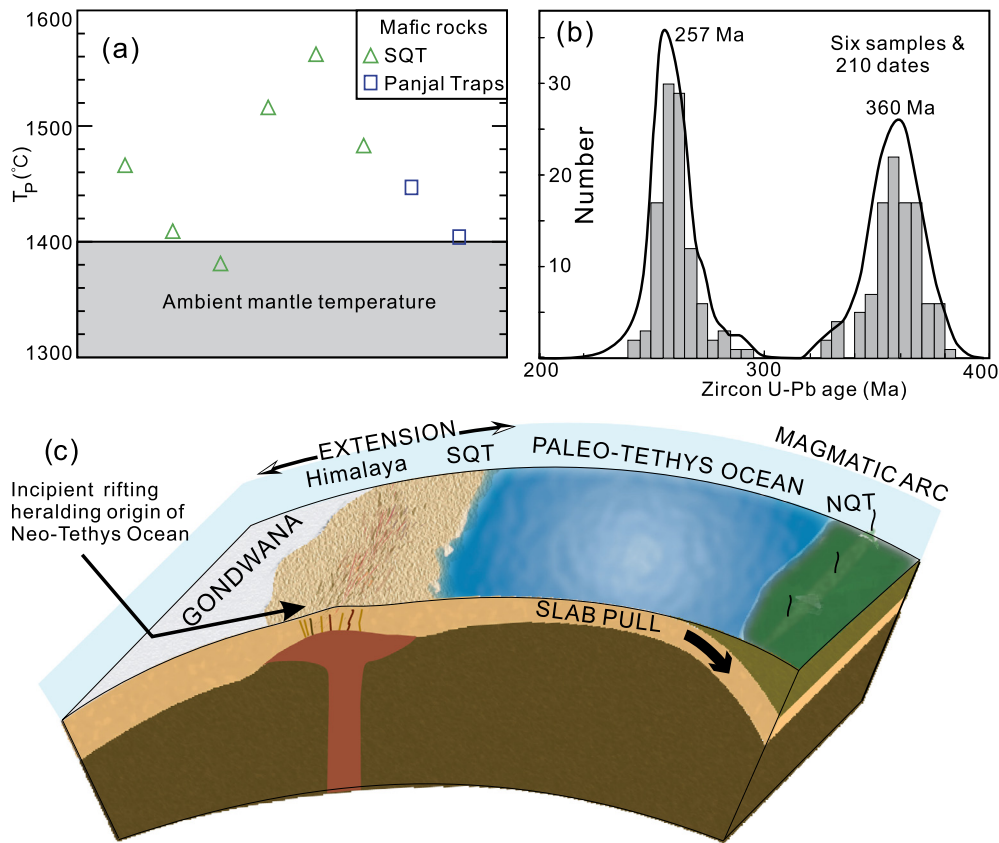
Fig. 4. The QP-LIP generated by combined slab pull and mantle plume. (a) High mantle potential temperatures for mafic rocks in the QP-LIP. (b) Detrital zircon age spectra from Carboniferous-Triassic strata in the NQT indicate renewed subduction of the Paleo-Tethys in Early Permian. (c) Cartoon illustrating the generation mechanism of the QP-LIP. Date and detailed references for (a) and (b) are provided in Table 1 and Table S5, respectively.

which become progressively thinner from west to east across the Himalaya (e.g., Garzanti et al., 1999; Zhu et al., 2010; Shellnutt, 2018), and are thickest in western Kashmir (Panjal Traps). In the east Cimmerian terranes, the thickness of basalts/sills decreases eastward from Southern Qiangtang (average of ~ 800 m with maximum of 2000 m) through Baoshan-Sibumasu ($\sim 300 - 500$ m) to the Lhasa terrane (< 100 m) (Zhu et al., 2010; Liao et al., 2015; Zhang and Zhang, 2017). Thus, we suggest the center of the QP-LIP was located NW of the present Indian plate, and that mafic lavas flowed to the north (SQT) and east (east Himalaya). We predict that QP-LIP should extend westward into the Pamir and adjacent terranes, but more studies, especially precise dating, are needed to test this model.

5.3. Combined slab pull forces and mantle plume to generate the QP-LIP

Two models have been proposed for the generation of the QP-LIP, including passive rifting (Gutiérrez-Alonso et al., 2008; Yeh and Shellnutt, 2016; Shellnutt, 2018) and the result of a mantle plume (e.g., Zhai et al., 2013; Liao et al., 2015; Wang et al., 2019). After the Paleo-Tethys mid-ocean ridge was subducted in the Late Carboniferous-Early Permian, slab pull forces could then be transmitted across the ocean basin and may have been responsible for rifting of the Cimmerian microcontinents from Gondwana during Early Permian (Stampfli and Borel, 2002; Gutiérrez-Alonso et al., 2008). On the other hand, many researchers have interpreted the mafic rocks from the QP-LIP to reflect the emplacement of a mantle plume based on their geochemical similarity with ocean island basalts (e.g., Chauvet et al., 2008; Zhai et al., 2013; Liao et al., 2015).

Recent geodynamic models suggest that these two models are not mutually exclusive and may act in concert. Lithospheric ex-

tension induced by slab pull forces would result in passive rifting along pre-existing lineaments along the northern Gondwana margin (e.g., Gutiérrez-Alonso et al., 2008). On the other hand, plumes emanating from the margins of a sub-Pangean LLSVP would have preferentially exploited lineaments where lithospheric extension occurred. Plume push is a strong but transient force (e.g., Zhang et al., 2018; Mitchell et al., 2021) and so is likely to be more significant in the early development of ocean basins. Slab pull, once subduction begins, on the other hand, is longer-lasting and may become the dominant force as these oceans widen.

The short ($\sim 290 - 285$ Ma) duration of emplacement of QP-LIP is typical of a mantle plume-produced LIP (Bryan and Ernst, 2008; Ernst, 2014). The mantle plume model is strongly supported by the high mantle potential temperatures (T_p) obtained from the mafic rocks. Eight samples, including two basalts from Panjal Traps and 6 mafic dikes from the SQT (Table 1), from presently available whole rock data, satisfy the requirement of being using sufficiently primitive to estimate T_p using PRIMELT3 software (Herzberg and Asimow, 2015). Five samples have previously been calculated T_p (Yeh and Shellnutt, 2016), and the remaining 3 new samples from the SQT are mafic dikes with similar texture to other mafic dikes used to calculated T_p successfully, with only a few olivine grains occurring in the picritic dike (MG708) (Zhai et al., 2013). The results show a large range of T_p ($\sim 1380 - 1560\,^\circ C$) (Table 1; Fig. 4a), indicating heterogeneity among samples or lithospheric contamination (e.g., Zhai et al., 2013; Shellnutt et al., 2015). The lithospheric contamination is reflected in the Th/Nb ratios (crustal input proxy, Pearce et al., 2021). The hottest rocks in the SQT have low Th/Nb (0.21-0.25) compared with the calculated values in the Panjal Traps (0.31-0.57) (Table 1), suggesting lithospheric contamination lowered their temperatures. But the maxima T_p of $\sim 1450 - 1560\,^\circ C$

Table 1

Mantle potential temperatures (T_p) of mafic rocks from the QP-LIP.

Sample	E713[#]	E801[#]	MG706[#]	MG707	MG708	13GZ82-3	PJ2-003[#]	PJ4-006[#]
Location	SQT	SQT	SQT	SQT	SQT	SQT	Panjal Traps	Panjal Traps
Whole rock geochemistry								
SiO_2	48.02	49.2	52.11	48.2	47.0	49.51	51.23	52.14
TiO_2	1.74	1.1	1.59	1.7	1.2	1.88	0.76	0.98
Al_2O_3	14.49	17.3	11.03	10.6	8.4	13.68	14.7	12.37
FeO^* (total)	9.09	8.44	7.66	10.53	11.0	9.61	8.35	7.82
MnO	0.15	0.1	0.16	0.2	0.2	0.15	0.15	0.15
MgO	8.26	8.78	8.8	14.23	19.75	9.10	7.5	7.37
CaO	11.74	11.70	11.9	10.54	9.18	11.93	12.24	11.9
Na_2O	2.27	2.05	2.49	1.66	0.76	2.04	1.33	3.25
K_2O	0.47	0.28	0.83	0.57	0.53	0.53	0.07	0.43
P_2O_5	0.20	0.11	0.17	0.15	0.10	0.16	0.08	0.07
Th/Nb	0.21	0.26	0.47	0.25	0.21	0.21	0.57	0.31
Calculated accumulated fractional primary melts and temperatures								
% olivine addition	21.25	13.81	10.15	10.93	−0.78	21.61	21.52	16.63
SiO_2	47.99	48.42	52.55	48.14	47.91	48.30	50.65	51.94
TiO_2	1.47	0.96	1.49	1.52	1.27	1.54	0.64	0.86
Al_2O_3	12.17	15.22	10.30	9.68	8.58	11.20	12.32	10.87
Fe_2O_3	0.85	0.82	0.79	1.07	1.25	0.87	0.78	0.76
FeO	8.90	8.02	7.42	9.57	10.10	9.12	8.47	7.82
MnO	0.16	0.15	0.17	0.16	0.17	0.16	0.16	0.16
MgO	16.10	13.93	12.88	18.07	19.86	16.77	15.45	13.80
CaO	9.90	10.33	11.14	9.63	9.42	9.80	10.30	10.49
Na_2O	1.90	1.80	2.32	1.51	0.78	1.67	1.11	2.85
K_2O	0.39	0.24	0.77	0.52	0.55	0.43	0.06	0.38
P_2O_5	0.17	0.10	0.16	0.14	0.11	0.13	0.07	0.06
T (°C)	1368	1321	1305	1403	1429	1378	1342	1330
T_P (°C)	1464	1407	1379	1514	1560	1481	1447	1404

Note: (1) Samples E713, E801, MG706, MG707, MG708 are from Zhai et al., 2013; 13GZ82-3 from this study; PJ2-003 from Shellnutt et al., 2014; PJ4-006 from Shellnutt et al., 2015. (2) The primary melt temperature (T) and mantle potential temperature (T_p) are calculated based on PRIMELT3 (Herzberg and Asimow, 2015). (3) Fe^{2+}/Fe^* is set to 0.9, leaving Fe_2O_3/TiO_2 blank. This suggestion is supported by the FeO^* enriched in the plot of FeO^* vs. MgO (Fig. S4). (4) Samples with [#] were previously calculated by Yeh and Shellnutt (2016), and our results are same. T_p for samples MG707, MG708 and 13GZ82-3 are new calculations and yield high T_p.

are significantly higher than the $\sim 1350 \pm 50\,°C$ for ambient mantle, consistent with a mantle plume involvement in the generation of this LIP.

This variation in the T_p among terranes is consistent with the large range of Nd isotopic values with slight differences in ranges between terranes (Fig. 5). The isotopic signature of basalts in continental LIPs can be influenced by a wide variety of sources (cf. Ernst, 2014). Basalts derived from melting of either deep mantle or asthenospheric mantle inherit the positive Nd signatures of their respective sources. However, negative isotopic signatures in basalts can be derived from a previously metasomatized sub-continental lithospheric mantle that has been resident beneath stable continents for long periods (Murphy and Dostal, 2007). Significant crustal contamination also tends to drive Nd isotopic compositions towards negative values (e.g., high SiO_2 samples in Fig. 5a). Thus, the Nd isotopic compositions of basalts in subdomains of a LIP are typically compositionally variable, especially along a continental margin where the mantle lithosphere is commonly heterogeneous due to previous tectonothermal activity, such as Kao LIP (e.g., Ellam et al., 1992). These variable sources are evident on the new LIP discrimination diagram (Fig. 5c), which shows most basalts plotting in a diagonal array from subduction-modified lithospheric mantle to mantle plume sources, implying significant lithosphere-plume interaction (Pearce et al., 2021). Although determining the relative importance of each of the aforementioned processes requires further study, we attribute the contrast of the predominantly negative Nd isotopic signature in the Himalaya, Baoshan and Lhasa terranes with the predominantly positive Nd isotopic signature in the SQT to such effects. For example, the SQT is a microcontinent lacking ancient thick lithosphere (Dan et al., 2020), whereas the Himalaya is part of the India Craton with thick and ancient lithosphere. In addition, the presence of ancient lithosphere has been documented

in the Lhasa and Baoshan terranes (e.g., Zhu et al., 2010; Metcalfe, 2013). Despite the potential influence of these heterogeneities, the younger phase (~ 285 Ma) has a more depleted mantle source than the older phase (~ 290 Ma) both in the SQT (Zhai et al., 2013; Xu et al., 2016) and the Panjal Traps (Shellnutt et al., 2015). This systematic variation with time suggests the change to more depleted Nd isotopic signature of basalts in the subdomains of the QP-LIP was controlled by a change in geodynamic setting that affected the entire region.

Renewed subduction along the northern margin of the eastern Paleo-Tethys Ocean in the Early Permian is indicated by the detrital zircon spectra of Carboniferous-Triassic strata (Zhang et al., 2017; Fig. 4b), and by recently documented Early Permian subduction-related magmatism in the Northern Qiangtang terrane (Song et al., 2017). The presence of post-Early Permian normal subduction-related rock assemblages in the eastern Paleo-Tethys realm (Northern Qiangtang-Indochina terranes) (Song et al., 2017; Wang et al., 2018; Xu et al., 2020) argues against oceanic ridge subduction during this time interval, which can result in abnormal geochemistry (summarized in Wang et al., 2020). These relationships imply that the mid-ocean ridge was subducted beneath Laurasia only in the western portion of the Paleo-Tethys realm, as interpreted from the Hellenides to Carpathians in the Late Carboniferous-earliest Permian (Gutiérrez-Alonso et al., 2008). In the aftermath of ridge subduction, slab pull forces associated with renewed subduction beneath Laurasia would have resulted in regional extension along the northern margin of Gondwana at the same time as plumes were ascending from the edges of the sub-Pangean LLSVP.

We speculate that slab pull forces created a regional extensional stress regime that reactivated inherently weak structures (e.g., previous sutures) between the Himalaya and Cimmerian microcontinents (Dan et al., 2020), where volcanism associated with
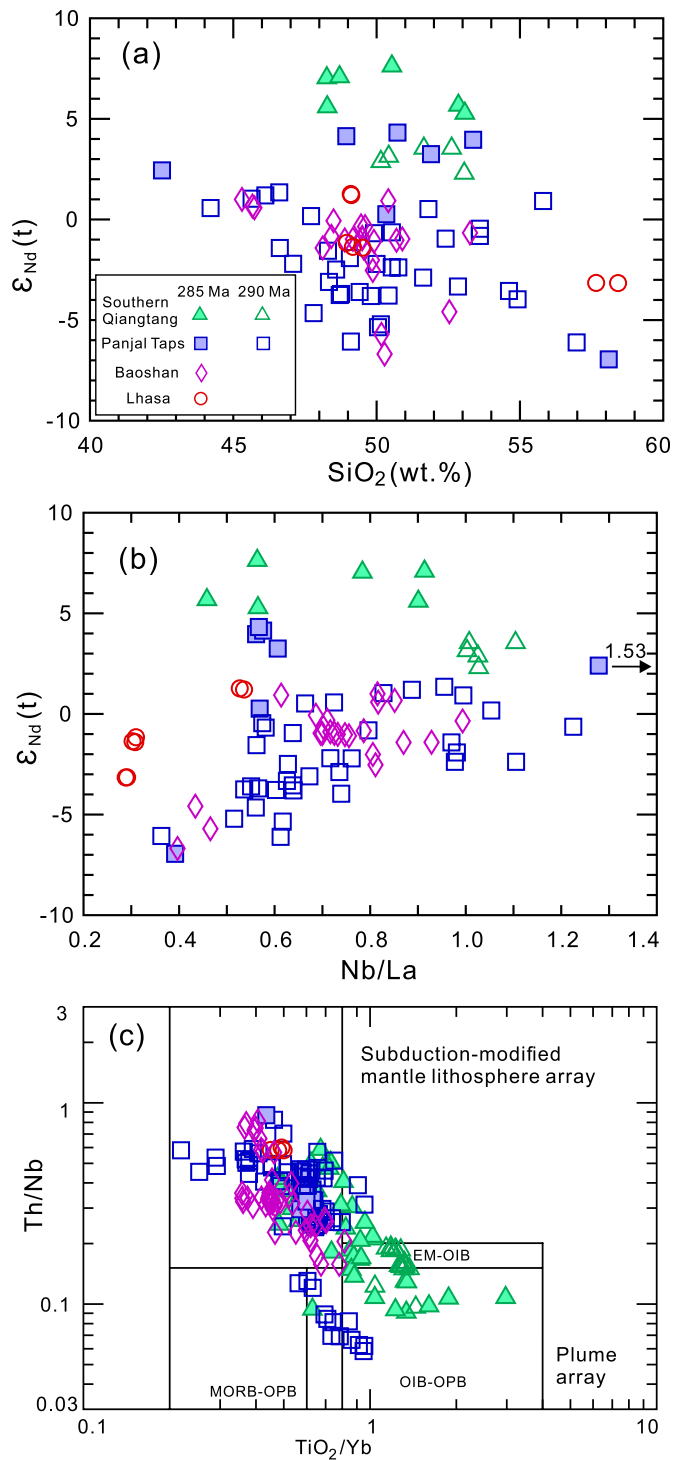
Fig. 5. Nd isotopes variation (a, b) and LIP discrimination diagram (c) (Pearce et al., 2021) for mafic rocks from in the QP-LIP. Data are from literatures: Southern Qiangtang (Zhai et al., 2013; Xu et al., 2016); Himalaya (Panjal Traps) (Chauvet et al., 2008; Shellnutt et al., 2014, 2015); Baoshan (Liao et al., 2015; Liu et al., 2020); Lhasa (Zhu et al., 2010). The samples in Baoshan and Lhasa are assumed to be formed ∼ 285 Ma based on this study.

the QP-LIP plume would have been localized and simultaneously promoted the rifting of east Cimmeria from the northern margin of Gondwana (Fig. 4c). The emplacement of the plume in the western Himalaya is responsible for the ∼ 290 Ma phase that is mainly focused in the Panjal Traps and is minor in the SQT, whereas the extension zone created by slab pull forces was responsible for the distribution of voluminous ∼ 285 Ma mafic rocks in the

Himalaya-Tibetan Plateau. The initial drift of Cimmeria from northern Gondwana coincided with the second igneous pulse (∼ 285 Ma) (syn-rift phase, see part 5.4) and subsequent drift was mostly likely due to the slab pull forces. These slab pull forces, normal to the northern Gondwanan margin, are also responsible for the ribbon shape of the Cimmerian microcontinents (Shellnutt, 2018), and for the margin-parallel syn-rift ∼ 285 Ma dike swarm in the SQT (Ernst, 2014).

Thus, a combination of slab pull forces and mantle plume magmatism may have initiated rifting the east Cimmerian microcontinents and opening of the Neo-Tethys Ocean. Among the five discovered Permian LIPs, i.e., ∼ 300 Ma Skagerrak-Centered LIP, ∼ 290 − 285 Ma QP-LIP, ∼ 290 − 270 Ma Tarim LIP, ∼ 260 Ma Emeishan LIP and ∼ 251 Ma Siberian Traps (cf. Ernst, 2014), only the QP-LIP is coeval with continent separation (Shellnutt, 2018). The QP-LIP was emplaced in a passive continental margin of the lower plate in a subduction system, in contrast to other Permian LIPs which were emplaced in inner part of major continents or in the upper plate of a subduction zone. Thus, many studies suggest the slab pull forces are responsible for rifting of the Cimmerian microcontinents and Neo-Tethys Ocean opening (Stampfli and Borel, 2002; Gutiérrez-Alonso et al., 2008; Shellnutt, 2018; Wan et al., 2019). However, our study implies that a short interval of magmatism along passive margin may have provided a transient force that initiated rifting but not necessarily continued to continent separation (Dan et al., 2021). The mantle plume would have helped to initiate the east Cimmerian microcontinents breakup, a proposal consistent the model of Buiter and Torsvik (2014) about the importance of pre-existing sutures in continental break-up.

5.4. Implication for birth of the Neo-Tethys Ocean

Biostratigraphic studies constrain the birth of the Neo-Tethys to the late Early Permian (e.g., Garzanti et al., 1994, 1996; Metcalfe, 1996, 2013), although the precise timing varies slightly among different studies. In the Tethyan Himalaya, a major unconformity in which late Sakmarian-Wuchiapingian strata (∼ 290 − 254 Ma) overlie either early Sakmarian (∼ 294 Ma) diamictites or Devonian-Carboniferous strata, is interpreted as breakup unconformity and constrained to the mid-Sakmarian (∼ 292 Ma) (Garzanti et al., 1996; Sciunnach and Garzanti, 2012). In the SQT, the 2-3 km thick Artinskian (290-283 Ma) turbidites are interpreted to reflect the tectonic separation of the SQT from Gondwana (Zhang et al., 2012). The separation of the Baoshan terrane from Gondwana is interpreted to have commenced just after emplacement of the ∼ 285 Ma Woniushi basalts (Wopfner, 1996). The several km thick late Sakmarian and mid-Artinskian Kaeng Krachan Group in Thailand (Sibumasu) and the Carnarvon Basin of Western Australia together imply a rift-to-drift transition during a similar time interval (Ridd, 2009). Although the opening the Neo-Tethys is probably diachronous, the widespread post-Artinskian Permian limestones in the SQT and Sibumasu are consistently interpreted as post-rift deposits (Ridd, 2009; Zhang et al., 2012).

Biostratigraphic data in combination with the U-Pb data presented herein suggest that the QP-LIP was emplaced slightly before and during the breakup of east Cimmerian microcontinents from Gondwana which heralded the opening of the Neo-Tethys (Fig. 3; e.g., Garzanti et al., 1999; Zhai et al., 2013; Shellnutt et al., 2015; Xu et al., 2016). The evolution of QP-LIP from ∼ 290 Ma alkali and tholeiitic basaltic, accompanied with crustally-derived silicic magmatism (Shellnutt et al., 2012), to ∼ 285 Ma tholeiitic compositions implies increasing degrees of partial melting and also decreasing depth of partial melting (e.g., Zhai et al., 2013; Shellnutt et al., 2015; Xu et al., 2016). The older phase occurred in the Himalaya and SQT around the center of the QP-LIP, whereas the younger phase occurred in almost every terrane that was undergo-

ing coeval rifting. The older pulse was related to initial continental rifting when the lithosphere was still thick, limiting the ascent of the plume, and consequently the volume of melt generated. However, the younger tholeiitic pulse occurred during the breakup event after lithospheric extension and thinning facilitated the rise of the plume to shallower depths which stimulated more voluminous melting.

The relationship between the ∼ 285 Ma breakup magmatism and the opening of the Neo-Tethys Ocean is indicated by the widespread distribution of tholeiitic basalts in the east Cimmerian microcontinents and Himalaya. This interpretation is consistent with the regional stratigraphy in which lower Permian basalts typically overlie syn-rift successions but underlie Middle-Upper Permian post-rift successions in the Himalaya (Garzanti et al., 1994, 1996, 1999). During the rift-to-drift transition, thick Artinskian (290-283 Ma) turbidites were deposited in the SQT (Zhang et al., 2012), and MORB (middle-ocean ridge basalt)-like basalts are reported in Panjal Traps (Shellnutt et al., 2015). Collectively, the stratigraphic, geochemical and geochronological data indicate that continental breakup is coeval with LIP magmatism (Buiter and Torsvik, 2014), analogous to the North Atlantic Igneous Province with a pre-rift phase (starting at ∼ 64 Ma) and a syn-rift phase (at ∼ 56 Ma) (e.g., Saunders et al., 1997; Wilkinson et al., 2017).

6. Conclusions

The Qiangtang-Panjal large igneous province (QP-LIP) is dominated by tholeiitic basalts with subordinate alkaline basalts. New SIMS zircon U-Pb ages for mafic rocks in the Southern Qiangtang terrane imply the QP-LIP was emplaced in a short time interval (290-285 Ma). Two phases of magmatism are recognized, a ∼ 290 Ma phase of minor alkalic and mainly tholeiitic basalts, and a voluminous and a regionally widespread ∼ 285 Ma phase that is dominated by tholeiitic basalt. Basalt compositions are consistent with a combination of subduction-modified lithospheric mantle and plume sources. The emplacement of QP-LIP was likely a combination of the arrival of a new mantle plume beneath the northern margin of Gondwana and slab pull-related extension which localized its emplacement. Generation of the QP-LIP was accompanied by rifting of the eastern Cimmerian microcontinents from the northern Gondwanan margin and opening of the Neo-Tethys.

CRediT authorship contribution statement

Wei Dan: Conceptualization, Formal analysis, Investigation, Methodology, Writing – original draft, Writing – review & editing. **Qiang Wang:** Conceptualization, Investigation, Methodology, Writing – review & editing. **J. Brendan Murphy:** Conceptualization, Writing – review & editing. **Xiu-Zheng Zhang:** Conceptualization, Formal analysis, Investigation, Writing – review & editing. **Yi-Gang Xu:** Conceptualization, Writing – review & editing. **William M. White:** Conceptualization, Writing – review & editing. **Zi-Qi Jiang:** Conceptualization, Formal analysis, Investigation, Writing – review & editing. **Quan Ou:** Conceptualization, Investigation, Writing – review & editing. **Lu-Lu Hao:** Conceptualization, Investigation, Writing – review & editing. **Yue Qi:** Conceptualization, Investigation, Writing – review & editing.

Declaration of competing interest

The authors declare that they have no known competing financial interests or personal relationships that could have appeared to influence the work reported in this paper.

Appendix A. Supplementary material

Supplementary material related to this article can be found online at https://doi.org/10.1016/j.epsl.2021.117054.

References

Bryan, S.E., Ernst, R.E., 2008. Revised definition of large igneous provinces (LIPs). Earth-Sci. Rev. 86, 175–202.

Buiter, S.J.H., Torsvik, T.H., 2014. A review of Wilson Cycle plate margins: a role for mantle plumes in continental break-up along sutures? Gondwana Res. 26, 627–653.

Burke, K., Steinberger, B., Torsvik, T.H., Smethurst, M.A., 2008. Plume generation zones at the margins of large low shear velocity provinces on the core-mantle boundary. Earth Planet. Sci. Lett. 265, 49–60.

Chauvet, F., Lapierre, H., Bosch, D., Guillot, S., Mascle, G., Vannay, J.C., Cotten, J., Brunet, P., Keller, F., 2008. Geochemistry of the Panjal Traps basalts (NW Himalaya): records of the Pangea Permian break-up. Bull. Soc. Géol. Fr. 179, 383–395.

Coffin, M.F., Eldholm, O., 1994. Large igneous provinces - crustal structure, dimensions, and external consequences. Rev. Geophys. 32, 1–36.

Dan, W., Wang, Q., Zhang, X.Z., Tang, G.J., 2020. Early Paleozoic S-type granites as the basement of Southern Qiangtang Terrane, Tibet. Lithos 356, 105395.

Dan, W., Wang, Q., White, W.M., Li, X.H., Zhang, X.Z., Tang, G.J., Ou, Q., Hao, L.L., Qi, Y., 2021. Passive-margin magmatism caused by enhanced slab-pull forces in central Tibet. Geology 49, 130–134.

Ellam, R.M., Carlson, R.W., Shirey, S.B., 1992. Evidence from Re-Os isotopes for plume-lithosphere mixing in Karoo flood basalt genesis. Nature 359, 718–720.

Ernst, R.E., 2014. Large Igneous Provinces. Cambridge University Press.

Flament, N., Williams, S., Muller, R.D., Gurnis, M., Bower, D.J., 2017. Origin and evolution of the deep thermochemical structure beneath Eurasia. Nat. Commun. 8, 14164.

Garzanti, E., Nicora, A., Tintori, T., Sciunnach, D., Angiolini, L., 1994. Late Paleozoic stratigraphy and petrography of the Thini Chu Group (Manang, Central Nepal): sedimentary record of Gondwana glaciation and rifting of Neotethys. Riv. Ital. Paleontol. Stratigr. 100, 155–194.

Garzanti, E., Angiolini, L., Sciunnach, D., 1996. The Permian Kuling Group (Spiti, Lahaul and Zanskar; NW Himalaya): sedimentary evolution during rift/drift transition and initial opening of Neo-Tethys. Riv. Ital. Paleontol. Stratigr. 102, 175–200.

Garzanti, E., Sciunnach, D., 1997. Early Carboniferous onset of Gondwanian glaciation and Neo-tethyan rifting in South Tibet. Earth Planet. Sci. Lett. 148, 359–365.

Garzanti, E., Le Fort, P., Sciunnach, D., 1999. First report of Lower Permian basalts in South Tibet: tholeiitic magmatism during break-up and incipient opening of Neotethys. J. Asian Earth Sci. 17, 533–546.

Gutiérrez-Alonso, G., Fernández-Suárez, J., Weil, A.B., Murphy, J.B., Nance, R.D., Corfu, F., Johnston, S.T., 2008. Self-subduction of the Pangaean global plate. Nat. Geosci. 1, 549–553.

Herzberg, C., Asimow, P.D., 2015. PRIMELT3 MEGA.XLSM software for primary magma calculation: peridotite primary magma MgO contents from the liquidus to the solidus. Geochem. Geophys. Geosyst. 16, 563–578.

Lapierre, H., Samper, A., Bosch, D., Maury, R.C., Bechennec, F., Cotten, J., Demant, A., Brunet, P., Keller, F., Marcoux, J., 2004. The Tethyan plume: geochemical diversity of Middle Permian basalts from the Oman rifted margin. Lithos 74, 167–198.

Li, X.H., Liu, X.M., Liu, Y.S., Su, L., Sun, W.D., Huang, H.Q., Yi, K., 2015. Accuracy of LA-ICPMS zircon U-Pb age determination: an inter-laboratory comparison. Sci. China Earth Sci. 58, 1722–1730.

Liang, D.Y., Nie, Z.T., Guo, T.Y., Xu, B.W., Zhang, Y.Z., Wang, W.P., 1983. Permo-Carboniferous Gondwana–Tethys facies in southern Karakoran Ali, Xizang (Tibet). Earth Sci. 19, 9–27 (in Chinese with English abstract).

Liao, S.Y., Wang, D.B., Tang, Y., Yin, F.G., Cao, S.N., Wang, L.Q., Wang, B.D., Sun, Z.M., 2015. Late Paleozoic Woniusi basaltic province from Sibumasu terrane: implications for the breakup of eastern Gondwana's northern margin. Geol. Soc. Am. Bull. 127, 1313–1330.

Liu, J., Wang, Q., Deng, J., Li, C., Li, G., Ripley, E.M., 2020. 280–310 Ma rift-related basaltic magmatism in northern Baoshan, SW China: implications for Gondwana reconstruction and mineral exploration. Gondwana Res. 77, 1–18.

Metcalfe, I., 1996. Gondwanaland dispersion, Asian accretion and evolution of eastern Tethys. Aust. J. Earth Sci. 43, 605–623.

Metcalfe, I., 2013. Gondwana dispersion and Asian accretion: tectonic and palaeogeographic evolution of eastern Tethys. J. Asian Earth Sci. 66, 1–33.

Mitchell, R.N., Zhang, N., Salminen, J., Liu, Y., Spencer, C.J., Steinberger, B., Murphy, J.B., Li, Z.-X., 2021. The supercontinent cycle. Nat. Rev. Earth Environ. 2, 358–374.

Murphy, J.B., Dostal, J., 2007. Continental mafic magmatism of different ages in the same terrane: constraints on the evolution of an enriched mantle source. Geology 35, 335–338.

Pearce, J.A., Ernst, R.E., Peate, D.W., Rogers, C., 2021. LIP printing: use of immobile element proxies to characterize Large Igneous Provinces in the geologic record. Lithos 392–393, 106068.

Rehman, H.U., Kitajima, K., Valley, J.W., Chung, S.L., Lee, H.Y., Yamamoto, H., Khan, T., 2018. Low-delta O-18 mantle-derived magma in Panjal Traps overprinted by hydrothermal alteration and Himalayan UHP metamorphism: revealed by SIMS zircon analysis. Gondwana Res. 56, 12–22.

Ridd, M.F., 2009. The Phuket Terrane: a Late Palaeozoic rift at the margin of Sibumasu. J. Asian Earth Sci. 36, 238–251.

Saunders, A.D., Fitton, J.G., Kerr, A.C., Norry, M.J., Kent, R.W., 1997. The North Atlantic Igneous Province. In: Mahoney, J.J., Coffin, M.F. (Eds.), Large Igneous Provinces: Continental, Oceanic, and Planetary Flood Volcanism. In: Geophysical Monographs. American Geophysical Union, pp. 45–93.

Sciunnach, D., Garzanti, E., 2012. Subsidence history of the Tethys Himalaya. Earth-Sci. Rev. 111, 179–198.

Shellnutt, J.G., Bhat, G.M., Brookfield, M.E., Jahn, B.M., 2011. No link between the Panjal Traps (Kashmir) and the Late Permian mass extinctions. Geophys. Res. Lett. 38, L19308. https://doi.org/10.1029/2011GL049032.

Shellnutt, J.G., Bhat, G.M., Wang, K.-L., Brookfield, M.E., Dostal, J., Jahn, B.-M., 2012. Origin of the silicic volcanic rocks of the Early Permian Panjal Traps, Kashmir, India. Chem. Geol. 334, 154–170.

Shellnutt, J.G., Bhat, G.M., Wang, K.-L., Brookfield, M.E., Jahn, B.-M., Dostal, J., 2014. Petrogenesis of the flood basalts from the Early Permian Panjal Traps, Kashmir, India: geochemical evidence for shallow melting of the mantle. Lithos 204, 159–171.

Shellnutt, J.G., Bhat, G.M., Wang, K.L., Yeh, M.W., Brookfield, M.E., Jahn, B.M., 2015. Multiple Mantle Sources of the Early Permian Panjal Traps, Kashmir, India. Am. J. Sci. 315, 589–619.

Shellnutt, J.G., 2018. The Panjal Traps. In: Sensarma, S., Storey, B.C. (Eds.), Large Igneous Provinces from Gondwana and Adjacent Regions. In: Special Publications, vol. 463. Geological Society, London, pp. 59–86.

Singh, A.K., Chung, S.L., Bikramaditya, R., Lee, H.Y., Khogenkumar, S., 2020. Zircon U-Pb geochronology, Hf isotopic compositions, and petrogenetic study of Abor volcanic rocks of Eastern Himalayan Syntaxis, Northeast India: implications for eruption during breakup of Eastern Gondwana. Geol. J. 55, 1227–1244.

Song, P.P., Ding, L., Li, Z.Y., Lippert, P.C., Yue, Y.H., 2017. An early bird from Gondwana: paleomagnetism of Lower Permian lavas from northern Qiangtang (Tibet) and the geography of the Paleo-Tethys. Earth Planet. Sci. Lett. 475, 119–133.

Stampfli, G.M., Borel, G.D., 2002. A plate tectonic model for the Paleozoic and Mesozoic constrained by dynamic plate boundaries and restored synthetic oceanic isochrons. Earth Planet. Sci. Lett. 196, 17–33.

Torsvik, T.H., Smethurst, M.A., Burke, K., Steinberger, B., 2006. Large igneous provinces generated from the margins of the large low-velocity provinces in the deep mantle. Geophys. J. Int. 167, 1447–1460.

Wan, B., Wu, F., Chen, L., Zhao, L., Liang, X., Xiao, W., Zhu, R., 2019. Cyclical one-way continental rupture-drift in the Tethyan evolution: subduction-driven plate tectonics. Sci. China Earth Sci. 62, 2005–2016.

Wang, M., Li, C., Zeng, X.W., Li, H., Fan, J.J., Xie, C.M., Hao, Y.J., 2019. Petrogenesis of the southern Qiangtang mafic dykes, Tibet: link to a late Paleozoic mantle plume on the northern margin of Gondwana? Geol. Soc. Am. Bull. 131, 1907–1919.

Wang, Q., Tang, G.J., Hao, L.L., Wyman, D.A., Ma, L., Dan, W., Zhang, X.Z., Liu, J.H., Huang, T.Y., Xu, C.B., 2020. Ridge subduction, magmatism, and metallogenesis. Sci. China Earth Sci. 63. https://doi.org/10.1007/s11430-11019-19619-11439.

Wang, X.D., Ueno, K., Mizuno, Y., Sugiyama, T., 2001. Late Paleozoic faunal, climatic, and geographic changes in the Baoshan block as a Gondwana-derived continental fragment in southwest China. Palaeogeogr. Palaeoclimatol. Palaeoecol. 170, 197–218.

Wang, Y., Qian, X., Cawood, P.A., Liu, H., Feng, Q., Zhao, G., Zhang, Y., He, H., Zhang, P., 2018. Closure of the East Paleotethyan Ocean and amalgamation of the Eastern Cimmerian and Southeast Asia continental fragments. Earth-Sci. Rev. 186, 195–230.

Wilkinson, C.M., Ganerød, M., Hendriks, B.W.H., Eide, E.A., 2017. Compilation and appraisal of geochronological data from the North Atlantic Igneous Province (NAIP). In: Péron-Pinvidic, G., Hopper, J.R., Stoker, M.S., Gaina, C., Doornenbal, J.C., Funck, T., Árting, U.E. (Eds.), The NE Atlantic Region: A Reappraisal of Crustal Structure, Tectonostratigraphy and Magmatic Evolution. In: Special Publications, vol. 447. Geological Society, London, pp. 69–103.

Wopfner, H., 1996. Gondwana origin of the Baoshan and Tengchong terranes of west Yunnan. In: Hall, R., Blundell, D. (Eds.), Tectonic Evolution of Southeast Asia. In: Special Publications, vol. 106. Geological Society, London, pp. 539–547.

Wopfner, H., Jin, X.C., 2009. Pangea Megasequences of Tethyan Gondwana-margin reflect global changes of climate and tectonism in Late Palaeozoic and Early Triassic times—a review. Palaeoworld 18, 169–192.

Wu, F.Y., Wan, B., Zhao, L., Xiao, W.J., Zhu, R.X., 2020. Tethyan geodynamics. Acta Petrol. Sin. 36, 1627–1674.

Xu, W., Dong, Y.S., Zhang, X.Z., Deng, M.R., Zhang, L., 2016. Petrogenesis of high-Ti mafic dykes from Southern Qiangtang, Tibet: implications for a ca. 290 Ma large igneous province related to the early Permian rifting of Gondwana. Gondwana Res. 36, 410–422.

Xu, W., Liu, F., Dong, Y., 2020. Cambrian to Triassic geodynamic evolution of central Qiangtang, Tibet. Earth-Sci. Rev. 201, 103083.

Yeh, M.W., Shellnutt, J.G., 2016. The initial break-up of Pangaea elicited by Late Palaeozoic deglaciation. Sci. Rep. 6, 31442. https://doi.org/10.1038/srep31442.

Zhai, Q.G., Jahn, B.M., Su, L., Ernst, R.E., Wang, K.L., Zhang, R.Y., Wang, J., Tang, S.H., 2013. SHRIMP zircon U-Pb geochronology, geochemistry and Sr-Nd-Hf isotopic compositions of a mafic dyke swarm in the Qiangtang terrane, northern Tibet and geodynamic implications. Lithos 174, 28–43.

Zhang, N., Dang, Z., Huang, C., Li, Z.X., 2018. The dominant driving force for supercontinent breakup: plume push or subduction retreat? Geosci. Front. 9, 997–1007.

Zhang, X.Z., Dong, Y.S., Wang, Q., Dan, W., Zhang, C.F., Xu, W., Huang, M.L., 2017. Metamorphic records for subduction erosion and subsequent underplating processes revealed by garnet-staurolite-muscovite schists in central Qiangtang, Tibet. Geochem. Geophys. Geosyst. 18, 266–279.

Zhang, Y.-c., Shen, S.-z., Shi, G.R., Wang, Y., Yuan, D.-x., Zhang, Y.-j., 2012. Tectonic evolution of the Qiangtang Block, northern Tibet during the Late Cisuralian (Late Early Permian): evidence from fusuline fossil records. Palaeogeogr. Palaeoclimatol. Palaeoecol. 350–352, 139–148.

Zhang, Y.X., Zhang, K.J., 2017. Early Permian Qiangtang flood basalts, northern Tibet, China: a mantle plume that disintegrated northern Gondwana? Gondwana Res. 44, 96–108.

Zhu, D.C., Mo, X.X., Zhao, Z.D., Niu, Y.L., Wang, L.Q., Chu, Q.H., Pan, G.T., Xu, J.F., Zhou, C.Y., 2010. Presence of Permian extension- and arc-type magmatism in southern Tibet: paleogeographic implications. Geol. Soc. Am. Bull. 122, 979–993.

Zhu, D.C., Zhao, Z.D., Niu, Y., Dilek, Y., Mo, X.X., 2011. Lhasa terrane in southern Tibet came from Australia. Geology 39, 727–730.